MODELLING FREE WATER IN DIFFUSION MRI

Emmanuel Vallée[1], Gwenaëlle Douaud[1], Andreas U Monsch[2], Achim Gass[3], Wenchuan Wu[1], Stephen M Smith[1], and Saad Jbabdi[1]
[1]*FMRIB, University of Oxford, Oxford, Oxfordshire, United Kingdom,* [2]*Memory Clinic, University Center for Medicine of Aging Basel, Basel, Switzerland,* [3]*Department of Neurology, University Hospital Mannheim, Heidelberg, Germany*

Purpose: Diffusion Tensor Imaging (DTI) is widely used in clinical neuroimaging research to infer microstructural alterations of white matter in pathologies or aging. As comparisons of DTI measures across subjects are often performed on a voxel-wise basis, the outcome can be sensitive to Partial Volume Effects (PVE), where a voxel represents a weighted average of different tissue types. This effect is widely present in DTI because of its relatively low resolution and the proximity of White Matter (WM) to ventricles filled with Free Water (FW). We propose here to model the contribution of FW to DTI data on a voxel-wise basis to retrieve unbiased microstructural properties of WM and to estimate the volume fraction of each compartment.

Method: We use a two compartments model that accounts for fast and slow diffusing water characterizing FW and tissue respectively[1]. Such a model can be written as $S_i = S_F e^{-b_i D_F} + S_T e^{-b_i \, {}^T_i \, \mathbf{r}_i}$, where S_i is the signal corresponding to the i^{th} diffusion gradient direction along direction r_i with b-value b_i, S_F and S_T are the signals from FW and Tissue compartments respectively, D_F is the diffusivity of free water, set to $0.003 mm^2.s^{-1}$ and D is the diffusion tensor. The FW Fraction (FWF) is given by $FWF = \frac{\hat{S}_F}{\hat{S}_F + \hat{S}_T}$, where $\hat{S}_T$ and $\hat{S}_F$ are the signals from tissue and FW corrected to account for the different relaxation times. The correction is computed using $S_X = \hat{S}_X(1 - e^{-\frac{TR}{T_{1,X}}})e^{-\frac{TE}{T_{2,X}}}$, where T_1/T_2 are fixed to typical values at 3T (FW: 3000/1000ms, WM: 800/80ms). Unlike previously proposed[2], we do not use spatial regularization to constrain our model, but put a prior on mean diffusivity (MD) for the tissue compartment. The mean and standard deviation of the prior were set to 7.10^{-4} and $1.10^{-4} mm^2.s^{-1}$. We also assess the benefits of using multi-shell data with low b-value (300s/mm^2) where the signal from fast diffusing FW is not fully attenuated. The fitting procedure is performed via sampling of the posterior distribution of all parameters using the Metropolis-Hastings algorithm. We first validate our approach through simulations, where we compare a single compartment tensor fit with our model fit performed with or without a prior on MD and on single or two-shell data (b=300/1000s.mm^{-2}). We then evaluate our model in-vivo by comparison with Inversion Recovery (IR) data, where FW signal was nulled using an inversion pulse. Data were acquired on a 3T Siemens Verio MR scanner, at 2mm isotropic resolution, with TE/TR=76/9600ms and TR=20600ms, TI=2300ms for the IR acquisition, with 60 b=1000s.mm^{-2} and 6 b=0 images. Also, to evaluate the impact of FW modelling in a clinical setting, we performed a preliminary TBSS analysis of 54 Alzheimer's Disease (AD) patients and 60 healthy elderly participants[3] The DWI data were acquired on a 3T MR scanner (TR/TE=7000/89ms), 2.5mm isotropic voxels, with 60 directions with b= 900s.mm^{-2} and six b=0.

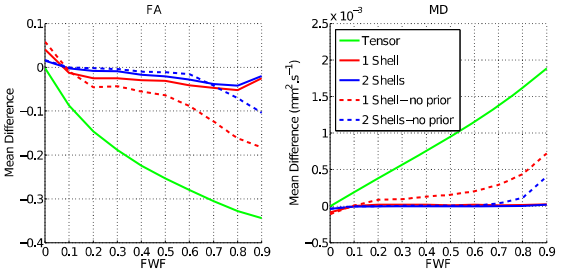

Figure 1: Comparison of FA and MD estimated by our model and with simple tensor

Tensor, IR and FW Results: Figure 1 shows simulation results, in terms of mean difference between the estimates of FA/MD and the true simulated values. As the FWF increases, the single compartment tensor fit underestimates FA and overestimates MD, which is the behaviour described in[4]. With the FW model, both FA and MD values are closer to the ground truth than the simple tensor fit, although the difference increases with FWF when the prior is not used. In the single shell case, the prior appears to be essential as the estimated FA and MD deviate from the ground truth, even at low FWF. When the fit is performed on the data with two shells, the prior has a less significant effect on the retrieval of the true values, suggesting that the second shell helps to constrain the fit.

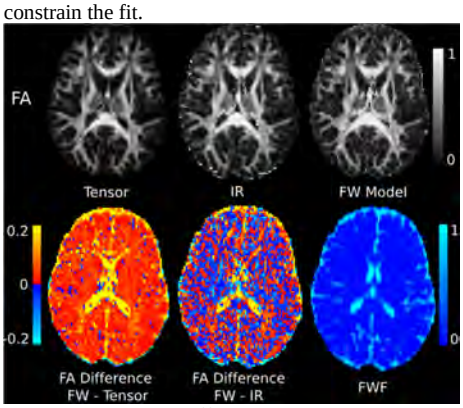

Figure 2: FA maps, differences between FW model, simple tensor and IR, and FWF map

Figure 2 ***(top)*** shows FA maps obtained with a single tensor, IR and FW model. In the simple tensor FA image (FA_{DTI}), the WM structures neighbouring the ventricles appear thinner and the voxels at the interface of WM and CSF have lower FA_{DTI} values than in the IR (FA_{IR}) and FW model (FA_{FW}) FA maps. In these voxels, both FA_{IR} and FA_{FW} values are consistent with the ones unaffected by Partial Voluming (PV). The corpus callosum and the fornix appear noticeably thicker and with higher intensity in both FA_{IR} and FA_{FW} maps. **Figure 2** ***(bottom)*** shows the difference in FA between the FW model, tensor and IR. Compared to FA_{DTI}, FA_{FW} increases everywhere in the brain. In comparison, only small differences can be seen between FA_{FW} and FA_{IR}. The FWF map in **Figure 2** ***(bottom)*** shows high values in the ventricles, intermediate ones in PV areas and, interestingly, values between 0.05 and 0.15 in WM, suggesting the presence of FW in deep white matter. **Table 1** gives a quantitative comparison of our model with IR, in terms of mean FA, MD and FWF in WM structures of interest. We can see that the values obtained with our model match the ones from the IR data. In accordance with simulations and[4], an increased FWF will result in a decreased FA_{DTI} and increased MD_{DTI}. Also, the tracts that are not in the vicinity of the ventricles (e.g., the cingulum and the SLF) still contain FW, which possibly in this case, reside in the extra-axonal space[2].

Tract Name	FA_{DTI}	FA_{IR}	FA_{FW}	MD_{DTI}	MD_{IR}	MD_{FW}	FWF
Cingulum	0.47	0.53	0.52	0.74	0.64	0.63	0.08
Corpus Callosum	0.66	0.74	0.76	0.87	0.70	0.67	0.11
Fornix	0.43	0.54	0.53	0.88	0.66	0.64	0.14
SLF	0.50	0.56	0.56	0.70	0.61	0.62	0.05

Table 1: FA and MD estimated by single tensor (DTI), IR and FW model (FW), and associated FWF

Preliminary FW Results in AD: TBSS analysis on AD showed widespread, significant decrease in FA_{DTI} for AD patients compared with healthy controls (**Figure 3,** ***top***), with an associated increase in MD_{DTI} (not shown)[3]. Next, the same TBSS analysis was carried out on FA_{FW}, MD_{FW} and FWF. Decrease in FA_{FW}, though present at a trend level, was no longer significant after correction for multiple comparisons, but we still observed a significant increase in MD_{FW} in the patients, albeit to a smaller extent than for MD_{DTI}; notably, there was a widespread, significant increase of FWF in the AD patients, in the same areas where a significant decrease in FA_{DTI} was observed (**Figure 3,** ***bottom***). These somewhat surprising results seem to suggest that the decreased FA_{DTI} typically observed in AD could be partly due to an increased FWF. Further work will be needed to determine whether such increase in FWF in AD might be due to macroscopic atrophy of the relevant WM tracts, to pathophysiological changes of the underlying WM tissue (such as an increase in the extra-axonal space, which is thought to be a marker of neuro-inflammation[5]), or to both.

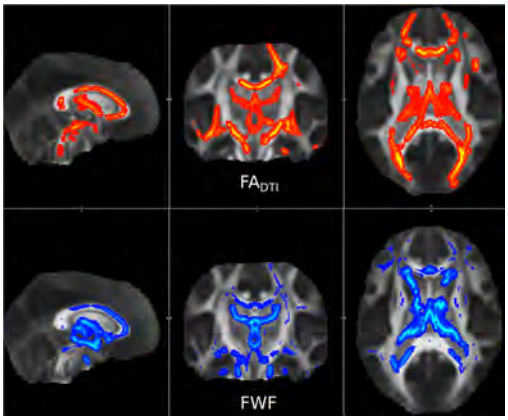

Figure 3: FA_{DTI} decrease and FWF increase in patients compared with healthy controls (TFCE corrected p<0.05)

Conclusion: We present here a model that accounts for free-water partial voluming in diffusion MRI and that is applicable to clinical data with single shell. The fit is performed voxel-wise, without spatial regularization and constrained by a prior on the tensor mean diffusivity. Using an extra shell with low b-value allows to relax this prior. Future efforts will focus towards understanding the contribution of tract atrophy and increased extra-axonal space to changes in WM FWF (e.g., using a geometric model of WM tracts) and FA_{FW}.

References: [1] Pierpaoli et al., ISMRM **12**:1215 (2004) – [2] Pasternak et al., MRM **62**:717 (2009) – [3] Douaud et al., Neuroimage **55**:880 (2011) – [4] Alexander et al., MRM **5**:770 (2001) - [5] Pasternak et al., J. Neuroscience **48**:17365 (2012)